ACS APPLIED MATERIALS & INTERFACES

Research Article

www.acsami.org

Modulated Charge Injection in p-Type Dye-Sensitized Solar Cells Using Fluorene-Based Light Absorbers

Zonghao Liu,[†] Dehua Xiong,[†] Xiaobao Xu,[†] Qudsia Arooj,[‡] Huan Wang,[†] Liyuan Yin,[†] Wenhui Li,[†] Huaizhi Wu,[†] Zhixin Zhao,[†,*] Wei Chen,[*,†] Mingkui Wang,[†] Feng Wang,[‡] Yi-Bing Cheng,[†,§] and Hongshan He[*,∥]

[†]Michael Grätzel Center for Mesoscopic Solar Cells, Wuhan National Laboratory for Optoelectronics and School of Optical and Electronic Information, Huazhong University of Science and Technology, Wuhan 430074, P. R. China

[∥]Department of Chemistry, Eastern Illinois University, Charleston, Illinois 61920, United States

[§]Department of Materials Engineering, Monash University, Melbourne, Victoria 3800, Australia

[‡]Molecular Model Discovery Laboratory, School of Science, Faculty of Science, Engineering and Technology, Swinburne University of Technology, Melbourne, Victoria 3122, Australia

Supporting Information

ABSTRACT: In this study, new pull−push arylamine-fluorene based organic dyes zzx-op1, zzx-op2, and zzx-op3 have been designed and synthesized for p-type dye-sensitized solar cells (p-DSCs). In zzx-op1, a di(p-carboxyphenyl)amine (DCPA) was used as an electron donor, a perylenemonoimide (PMID) as an electron acceptor, and a fluorene (FLU) unit with two aliphatic hexyl chains as a π-conjugated linker. In zzx-op2 and zzx-op3, a 3,4-ethylenedioxythiophene (EDOT) and a thiophene were inserted consecutively between PMID and FLU to tune the energy levels of the frontier molecular orbitals of the dyes. The structural modification broadened the spectral coverage from an onset of 700 nm for zzx-op1 to 750 nm for zzx-op3. The electron-rich EDOT and thiophene lifted up the HOMO (highest occupied molecular orbital) levels of zzx-op2 and zzx-op3, making their potential more negative than zzx-op1. When three dyes were employed in p-type DSCs with I^-/I_3^- as a redox couple and NiO nanoparticles as hole materials, zzx-op1 exhibited impressive energy conversion efficiency of 0.184% with the open-circuit voltage (V_{OC}) of 112 mV and the short-circuit current density (J_{SC}) of 4.36 mA cm^{-2} under AM 1.5G condition. Density functional theory calculations, transient photovoltage decay measurements, and electrochemical impedance spectroscopic studies revealed that zzx-op1 sensitized solar cell exhibited much higher charge injection efficiency (90.3%) than zzx-op2 (53.9%) and zzx-op3 (39.0%), indicating a trade-off between spectral broadening and electron injection driving force in p-type DSCs.

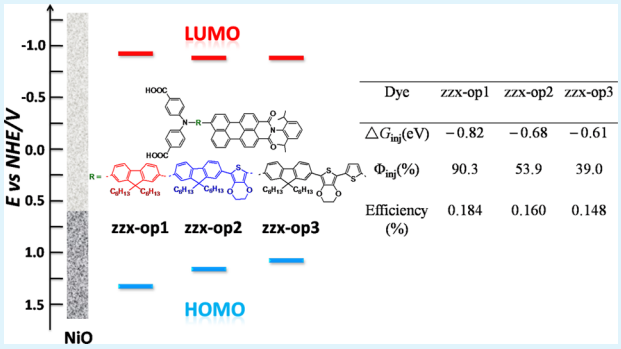

KEYWORDS: *p-type dye-sensitized solar cells, charge injection, organic sensitizer, fluorene, NiO*

INTRODUCTION

Conversion of sunlight to electricity is of importance to efficient utilization of abundant solar energy. Among many devices, dye-sensitized solar cells (DSCs) have emerged as a key technology in this field.[1] During the last two decades, extensive research has been carried out to make this technology cost-effective.[2−4] The major efforts have been devoted to n-type DSCs, in which dye-coated n-type TiO_2 nanoparticles are used. The dye molecules absorb the sunlight and inject the electrons to the conduction band of TiO_2 nanoparticles to produce electrons for external circuit.[5] Recently, energy conversion efficiency of 12.3% has been reported;[6] it is still challenging to construct dyes that are capable of harvesting photons in the visible and near-infrared regions. One strategy to overcome this limitation is to design tandem DSCs by stacking n-type and p-type electrodes together.[7−11] In tandems cells, two electrodes can be sensitized by complementary dyes, providing great opportunities to increase the conversion efficiency with low cost. To date, the best energy conversion efficiency from tandem DSCs is 2.42%,[8] which is far below the record of 12.3% efficiency[6] from a single n-type DSC. The lack of appropriate p-type semiconductor and dyes limits the overall photovoltaic performance of the devices. It is imperative to develop advanced materials for the p-type DSCs, including dyes and hole transport materials.[7,9]

Dyes with a push−pull configuration perform better than those without such a configuration in p-type DSCs.[12−18] Sun and co-workers[19−21] synthesized triphenylamine-based push−

Received: December 6, 2013
Accepted: February 12, 2014
Published: February 12, 2014

pull dyes for p-type DSCc and reported the energy conversion efficiency of 0.15%. Lin and co-workers[22,23] prepared arylamine-based organic dyes with two anchoring groups. They found the photon-to-current response extended to 700 nm. When thiophene derivatives were used as electron acceptors, energy conversion efficiency between 0.06 and 0.11% was obtained. Wu and co-worker[24] studied the linker effect on energy conversion efficiency in a series of donor−acceptor dyes. It was concluded that 3,4-ethylenedioxythiophene was a better linker than thiophene and phenyl groups because of the broader IPCE response. Udo and co-worker[8,25,26] found the efficiency increased to 0.41−0.61% when more thiophene units were added between donors and acceptors. Recently, the record efficiency of 1.3% was achieved by employing the tris(1,2-diaminoethane)cobalt (II/III) as an electrolyte and PMI-6T-TPA as a dye. In this dye, the linker consisted of six thiophene units.[27]

The charge transfer process is also important in p-type DSCs.[9] As shown in Figure 1, the light-harvesting efficiency

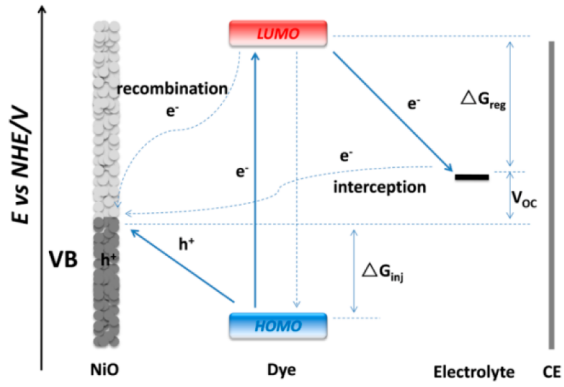

Figure 1. Schematic of charge transfer process in p-type DSCs, arrows with solid lines denote desired transfer for energy conversion, and those with dashed lines denote undesired transfer. The free energies of hole injection $\Delta G_{inj} = e[E_{VB} - E_{HOMO}]$, the free energies of dye regeneration $\Delta G_{reg} = e[E_{redox} - E_{LUMO}]$, the $V_{OCmax} = E_{redox} - E_{VB}$.[40]

(LHE), the hole injection quantum yield (Φ_{inj}), and the charge collection efficiency(η_{coll}) at the FTO electrode determine the incident photon to current conversion efficiency (IPCE) according to eq 1[28]

$$\text{IPCE} = \text{LHE} \times \Phi_{inj} \times \eta_{coll} \quad (1)$$

η_{coll} is the product of Φ_{esc} and η_{tr}.[28] The Φ_{esc} represents the escape quantum yield, which is the probability that an injected hole does not recombine with the reduced dye directly. It depends strongly on the regeneration rate of the reduced dye to its ground state by the electrolyte, and is dominated by the recombination between injected hole and reduced dye. Such recombination could be suppressed by using a secondary electron acceptor that is bound to the chromophore unit to populate the longer-lived charge separated state or by using a longer linker to extend the distance between the acceptor and the semiconductor. The transport efficiency η_{tr} is the probability that the hole reaches the conducting substrate, and is dominated by interception of the injected hole by the electrolyte causing high dark current.[28] In the I^-/I_3^- and NiO system, the dye structure exerts more pronounced impact on LHE and Φ_{inj}. Hagfeldt and co-workers[28] reported that the hole injection process was ultrafast in coumarin 343 (~200 fs)[29] and phosphorus porphyrin (2−20 ps) sensitized p-type DSCs. The hole injection driving force was 1.0 and 1.1 eV, respectively. The charge recombination between the injected hole and the reduced dye was very fast, causing significant loss of photocurrent and photovoltage. In addition, fast interfacial interception of the injected hole by the electrolyte also leads to high dark current.[9] Mori and co-workers[30] found that the absorbed photon-to-current conversion efficiency (APCE) increased with the increase of hole injection driving force. The APCE of 30% was obtained when the hole injection driving force reached 0.6 eV. Compared to extensive research on the electron injection kinetics mechanism for n-type DSCs, the study on hole injection for p-type DSCs is scarce.[31] It is still an open question how to modulate hole injection at the interface of NiO/dye/electrolyte for p-type DSCs through molecular engineering of dyes.

In this report, three new organic dyes with di(*p*-carboxy)-phenylamine as a donor and a perylenemonoimide as an electron acceptor were designed and synthesized to investigate how the linkers between a donor and an acceptor affect the charge injection efficiency. A fluorene, a 3,4-ethylenedioxythiophene(EDOT), and a thiophene were inserted between DCPA and PMID consecutively to tune the absorption spectra and the charge injection driving force. The structure of three dyes is shown in Scheme 1. The n-hexyl-substituted fluorene

Scheme 1. Structures of zzx-op1, zzx-op2, and zzx-op3

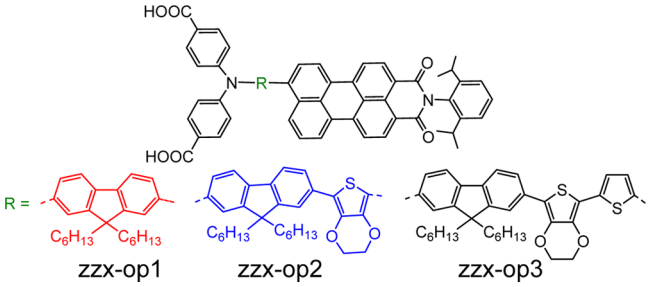

was chosen to construct the base structure because it has excellent hole transfer properties.[32,33] The aliphatic n-hexyl chains form a hydrophobic layer at the interface of NiO/dye/electrolyte, retarding the charge recombination between the injected holes and the electrolyte. We selected 3,4-ethylenedioxythiophene (EDOT)[34−36] and thiophene[37−39] as spacers because of their effective modulation of the frontier molecular energy of the dyes in organic solar cells and n-type DSCs for. It is expected that this design will tune the frontier molecular energy levels while exert the minimal influence of dye adsorption characteristics on the NiO films. Our results showed that the charge injection efficiency decreased in the order of zzx-op1 (90.3%) > zzx-op2 (53.9%) > zzx-op3 (39.0%), resulting in the decrease of the energy conversion efficiency in the order of zzx-op1 (0.184%) > zzx-op2 (0.160%) > zzx-op3 (0.148%). The results showed the importance of balancing the spectral broadening and charge injection driving force in order to obtain high energy conversion efficiency in p-type DSCs.

2. RESULTS AND DISCUSSION

Synthesis of the Dyes. Scheme 2 shows the synthesis of three dyes. The diphenylamine 1 was prepared from a Buchwald-Hartwig reaction in the presence of $Pd(OAc)_2$ and

dx.doi.org/10.1021/am405610b | ACS Appl. Mater. Interfaces 2014, 6, 3448−3454

Scheme 2. Synthesis of Push-Pull Dyes zzx-op1, zzx-op2, and zzx-op3

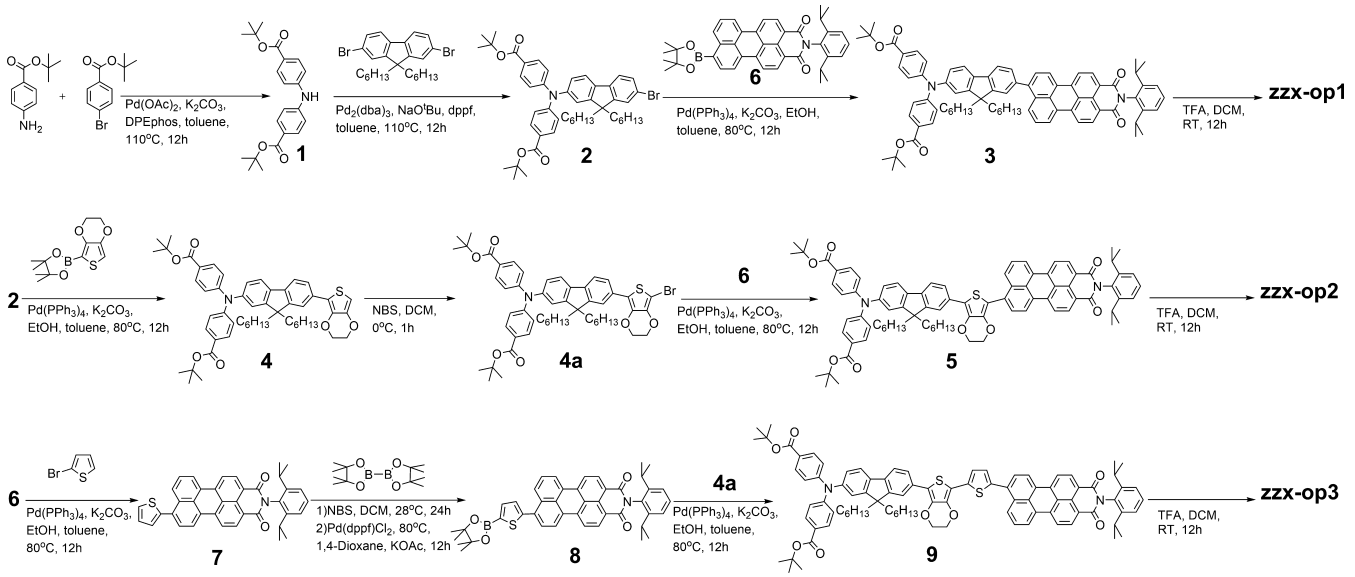

K_2CO_3 with an overall yield of 60%.[41] The diphenylamine-fluorene derivative 2 was obtained in a similar reaction in the presence of $Pd_2(dba)_3$ and a strong base NaO*t*-Bu in 42% yield. Compound 2 was reacted with a borate-perylenemonoimide derivative from a Pd-catalyzed Suzuki cross-coupling reaction and produced compound 3 in 83% yield. The compound 3 was then hydrolyzed in the presence of TFA in dry dichloromethane at 28 °C to give zzx-op1 in 94% yield.[41] The preparation of zzx-op2 started from compound 2. The 3,4-ethylenedioxythiophene was reacted with compound 2 under a similar Pd-catalyzed Suzuki cross-coupling conditions to give compound 4 in 54%.[42] Then it reacted with NBS at 0 °C to produce brominated compound 4a, which reacted with perylenemonoimide under the same Suzuki cross-coupling conditions to produce compound 5 in 86% yield. It was further hydrolyzed by TFA in dry dichloromethane to give zzx-op2 in 94% yield.[41] The preparation of zzx-op3 was different. The borate-thiophene-perylenemonoimide derivative 8 was first synthesized using a Pd-catalyzed borylation reaction in 13% yield.[43] Then compound 8 was reacted with compound 4a to give compound 9 in 39% yield, which was then hydrolyzed by TFA to give zzx-op3 in 92% yield. The structures and purity of all the intermediates and final compounds were identified by NMR and high resolution mass spectrometry (see the Supporting Information)

Absorption Spectra. Figure 2 shows the UV−vis absorption spectra of three dyes in THF. The photophysical data are summarized in Table 1. All three dyes show two major absorption bands in the range of 300−700 nm. The first band (~360 nm) comes from the linker and the donor group, whereas the second band (~520 nm) is attributed to the $\pi-\pi^*$ electron transition of acceptor.[41] Three dyes show very similar absorption coefficients ε; however, their absorption peak positions are quite different. The dye zzx-op1 has a maximum absorption wavelength of 521 nm. When a 3,4-ethylenedioxythiophene unit was inserted between the acceptor and FLU in zzx-op2, the absorption maximum red-shifted to 530 nm, which shifted further to 546 nm when an additional thiophene unit was added in zzx-op3. When these dyes were stained on NiO films, the spectra broadened compared to those in solution (see Figure S1 in the Supporting Information). The dye zzx-op3

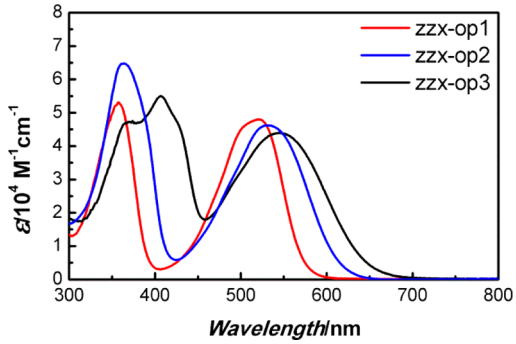

Figure 2. Absorption spectra of zzx-op1, zzx-op2, and zzx-op3 in THF.

exhibits a very broad absorption spectrum with an optical onset up to 750 nm. Three dyes showed very similar fluorescence spectra (see Figure S2 in the Supporting Information) with emission peaks centered at 650, 700, and 750 nm for zzx-op1, zzx-op2, and zzx-op3, respectively.

Photovoltaic Performance. The zzx-op1, zzx-op2, and zzx-op3 sensitized p-type DSCs were fabricated in a "sandwiched" configuration with I_3^-/I^- as a redox couple. The dyes were dissolved in THF/acetonitrile (v/v, 2/1) to reach the desired concentration for dye-loading.[44] The photovoltaic data are summarized in Table 2 and the typical *J*−*V* curves of the devices are shown in Figure 3. The open-circuit voltages (V_{OC}) and the fill-factors (FF) of three cells were quite similar to each other; whereas the short-circuit current densities (J_{SC}) were different. The J_{SC} decreased on the order of zzx-op1 > zzx-op2 > zzx-op3. The energy conversion efficiency also decreased in the order of zzx-op1 (0.184%) > zzx-op2 (0.160%) > zzx-op3 (0.148%). The zzx-op1 exhibited better photovoltaic performance than zzx-op2 and zzx-op3, which was contrary to its narrower absorption than other two as shown in Figure 2. The IPCE spectra, as shown in Figure 4, are consistent with their J_{SC}. The calculated J_{SC} values from the spectra were also quite close to those listed in Table 2, indicating the accuracy of the measurements. Three dyes showed very similar IPCEs from 360 to 380 nm with maximal values of 44, 48, and 42% for zzx-op1, zzx-op2, and zzx-op3,

Table 1. Optical and Electrochemical Data of Dyes zzx-op1, zzx-op2, and zzx-op3

dye	λ_{abs} [a] (nm) (ε ($\times 10^4$ M^{-1} cm^{-1}))	E_{ox} [b] (V, vs NHE)	E_{red} [b] (V, vs NHE)	ΔE_{0-0} [c] (ev)	ΔG_{inj} [d] (eV)	ΔG_{reg} (I^-/I_3^-) [e] (eV)	dye loading density (mol cm^{-2}) [f]
zzx-op1	357 (5.31), 521 (4.80)	1.28	−0.85	2.21	−0.82	−0.66	2.098×10^{-7}
zzx-op2	361 (6.47), 530 (4.62)	1.20	−0.82	2.04	−0.68	−0.63	2.100×10^{-7}
zzx-op3	407 (5.50), 545 (4.40)	1.10	−0.81	1.96	−0.61	−0.62	2.153×10^{-7}

[a]The absorption and emission spectra were measured in THF at room temperature. [b]The ground-state oxidation potential (E_{ox}) and reduction potential (E_{red}) of the dyes were measured in dry THF, and potentials measured vs ferrocene/ferrocenium (Fc/Fc^+) couple were converted to normal hydrogen electrode (NHE) by addition of +0.63 V. [c]The zero−zero transition energy ($E_{0-0}(S^*)$) was estimated from the intersection of normalized absorption and emission curves. [d]Calculated according to the equation:$\Delta G_{inj} = e[E_{VB}(NiO) - (E_{0-0}(S^*) + E_{red}(S/S^-))]$, $E_{VB}(NiO) = 0.54$ V vs NHE. [e]Calculated according to the equation: $\Delta G_{reg} = e[E(M/M^-) - E_{red}(S/S^-)]$, $E(I_3^-/I_2^{\cdot-}) = -0.19$ V vs NHE. [f]The dye-loaded photocathodes with an area 1.0 × 1.0 cm^2 and 2.3 μm thickness were immersed into 8 mL of 0.1 M NaOH methanol solution for 2 days under dark to deadsorb dye molecules. By comparing the UV−vis spectra of the desorbed dyes solution with different dye molecules (dye molecules dissolved in 0.1 M NaOH methanol solution with different concentration: 0.030, 0.015, 0.0075, 0.0050, and 0.00375 mM), the dye loading amounts of **zzx-op1-op3** on the NiO film (2.3 μm) were calculated.

Table 2. Photovoltaic Data of zzx-op1-op3 Sensitized Solar Cells under Illumination of 100 mW cm^{-2}, AM1.5G Condition

dye	V_{OC} (V)	J_{SC} (mA cm^{-2})	fill factor	efficiency (%)
zzx-op1	0.112	4.36	0.38	0.184
zzx-op2	0.111	4.00	0.36	0.160
zzx-op3	0.109	3.80	0.36	0.148

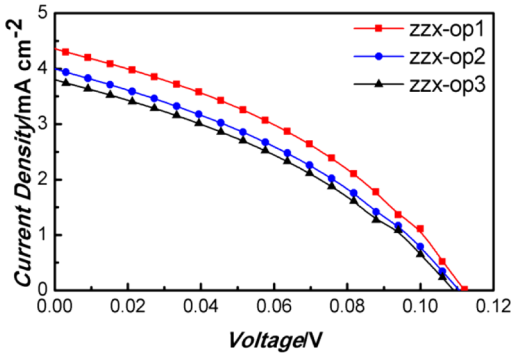

Figure 3. $J-V$ curves of zzx-op1, zzx-op2, and zzx-op3 sensitized solar cells.

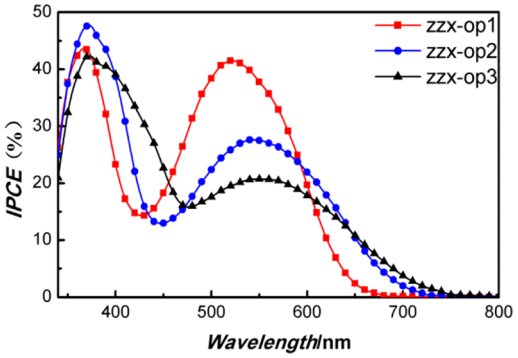

Figure 4. IPCE spectra of zzx-op1, zzx-op2, and zzx-op3 sensitized solar cells.

respectively. The zzx-op1 sensitized solar cell exhibited much higher IPCE than zzx-op2 and zzx-op3 from 450 to 600 nm. It should be noted that the IPCE spectra are not in agreement with the trend of their absorption spectra. The zzx-op2 and zzx-op3 with broader absorption did not result in better photovoltaic performance than zzx-op1. We determined the amounts of dye molecules on the NiO surface to reveal if such a discrepancy came from different dye-loading density. The results showed that three dyes had almost identical dye densities (Table 1). Therefore, different J_{SC} vales of three dyes with different linkers were not stemmed from their different adsorption capacities.[41]

Electrochemical Impedance Spectroscopy. The recombination between injected holes and reduced dye and electrolyte (interception process in Figure 1.) is responsible for the photocurrent losses in p-type DSCs under light illumination.[45] Under dark condition, the latter dominates the charge recombination process. The electrochemical impedance spectroscopy (EIS) was performed to investigate the charge recombination process in the devices. The photocathode/electrolyte interfacial charge transfer resistance, i.e., charge recombination resistance (R_{rec}), was calculated using a transmission line model.[45,46] Figure 5 showed the dependence

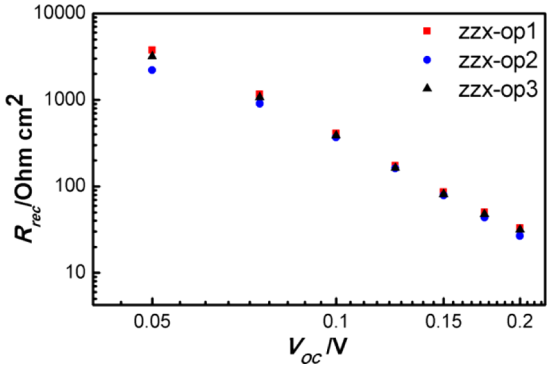

Figure 5. Interfacial charge recombination resistance (R_{rec}) as a function of applied bias obtained from electrochemical impedance measurements in the dark.

of R_{rec} on the applied bias in the dark. Nyquist plots of the devices under 125 mV bias in the dark were shown in Figure S4 in the Supporting Information, in which the diameters of semicircle for zzx-op1-op3 sensitized solar cells were nearly identical. These results indicated that the resistances against interfacial hole transfer from the NiO film to the reduced species in the electrolyte were almost the same, indicating nearly identical η_{tr} for three devices.[28,45]

Transient Photovoltage and Photocurrent Measurements. To further explore the cause of the discrepancy between absorption spectra and energy conversion efficiency, wee carried out transient photovoltage/photocurrent decay measurements to determine the hole lifetimes in the

devices.[47−49] Figure 6a shows the extracted charge density (n_t) of three devices under different light intensities. The charge

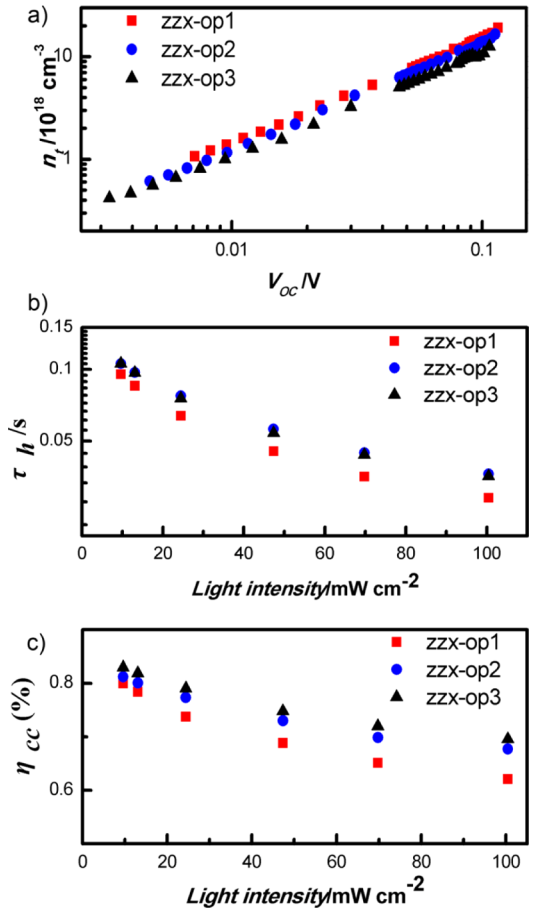

Figure 6. (a) Extracted charge density (n_t) vs V_{OC}, (b) hole lifetime (τ_h), and (c) (η_{cc}) charge collection efficiency vs incident light intensity for zzx-op1-op3 sensitized solar cells.

density for zzx-op1 is higher than those of zzx-op2 and zzx-op3, which matched the higher J_{SC} and IPCE of zzx-op1. Figure 6b shows the hole lifetime (τ_h) of devices as a function of light intensity. The τ_h of zzx-op1 sensitized solar cell is lower than those of zzx-op2 and zzx-op3 based devices, indicating the faster charge recombination in zzx-op1 sensitized solar cells. The hole lifetime (τ_h) represents the time of active holes survived from the recombination between injected holes and reduced dye and electrolyte.[49] The electrochemical measurements showed that zzx-op1-op3 sensitized solar cells exhibit nearly identical charge recombination between injected hole and electrolyte. Therefore, the different τ_h values of zzx-op1-op3 sensitized solar cells were attributed to the different charge recombination between injected hole and reduced dye.[28,30,45] Udo and co-workers[8] have reported that the charge recombination between injected hole and reduced dye can be effectively retarded by extending the molecule length. In our case, the zzx-op3 and zzx-op2 obviously showed longer molecule length than zzx-op1 because of additional EDOT and thiophene units as shown in Figure 7. The distance between the LUMO and NiO surface decreased in the order of zzx-op3 > zzx-op2 > zzx-op1. The shortest distance in zzx-op1 produced faster charge recombination, which gave the lowest τ_h.[8] Figure 6c showed the charge collection efficiency of devices

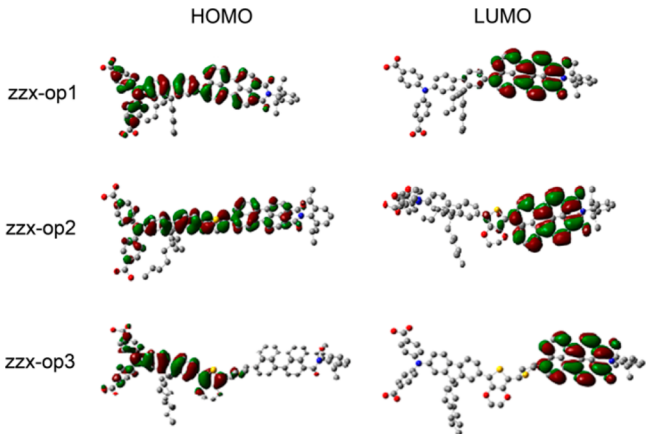

Figure 7. Geometry-optimized structures of zzx-op1-op3 and the electron density distribution of frontier molecular orbitals from DFT calculations with the B3LYP/6-311G(d) model.

under different light intensities. It was found that the zzx-op1 exhibited lower η_{cc} than other two dyes. This is due to the faster charge recombination for zzx-op1 than that of zzx-op2 and zzx-op3. This corresponded to the lower Φ_{esc} of zzx-op1 sensitized solar cells in eq 1.[28]

Theoretical Studies. The calculations were performed on density functional theory (DFT) level to reveal if the different photovoltaic performance of three dyes related to the structural conformation and electron density distribution.[50,51] Figure 7 shows the geometry-optimized structure and electron density distribution profiles of frontier molecular orbitals. The electron density distribution of three dyes on LUMOs (lowest unoccupied molecular orbitals) was quite similar to each other and was significantly localized on the PMID unit. The electron density distribution on HOMO (highest occupied molecular orbital) is quite different. In zzx-op1, the electron density is more pronounced in the donor section and is extended significantly to acceptor, PMID. In zzx-op2, the electron density in the donor reduced with concurrent increase on the FLU and extension to PMID unit. In both cases, a disjoint character was observed, which provides continuity of π-conjugation for charge injection. When an additional thiophene was added between EDOT and PMID, the HOMO of zzx-op3 is mainly localized on the linker. This nondisjoint character may also contribute its poor performance. Interestingly, the torsion angle of π-linkers and PMI are 56.66, 22.85, and 21.07° for zzx-op1-op3, respectively. The planarity between FLU and EDOT increased from zzx-op1, zzx-op2, to zzx-op3. The dihedral angle between PMID and FLU in zzx-op2 and PMID and thiophene in zzx-op3 increased from 48.00 to 89.57° in zzx-op3. As a result, the angles between PMID and FLU in three dyes are quite close to 60°. This indicated that interaction of dyes on the NiO may share a very close orientation because of similar geometry; therefore, dye aggregation (if any) should make the same contribution to the overall performance.

Electrochemical Properties. The cyclic voltammogram (CV) measurements in THF were performed to further explore the discrepancy in efficiency. The cyclic voltammogram (CV) is shown in Figure S3 in the Supporting Information. The first oxidation potentials (E_{ox}) and the first reduction potentials (E_{red}) are listed in Table 1. In p-type DSCs, the holes were injected into the valence band of semiconductor from the excited state of sensitizer leading to the reduction of sensitizer (S/S^-) upon light absorption. The hole injection driving force

can be determined according to the equation: ΔG_{inj} = e[E_{VB}(NiO) − (E_{0-0}(S*) + E_{red} (S/S$^-$))], where E_{VB}(NiO) = 0.54 V vs NHE. The measured E_{red} values were −0.85, −0.82, −0.81 V (vs NHE) for zzx-op1, zzx-op2, and zzx-op3, respectively. The hole injection driving forces were determined to be −0.82 ev (zzx-op1), −0.68 ev (zzx-op2), and −0.61 ev (zzx-op3), respectively. The differences were due to the different HOMO levels. As shown in Figure 8, the introduction

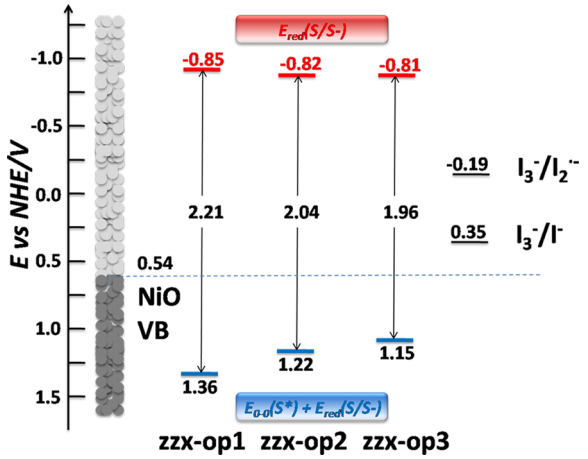

Figure 8. Energy diagram of zzx-op1, zzx-op2, and zzx-op3.

of electron-rich heterocyclic aromatic groups as linkers in zzx-op2 and zzx-op3 lifted the HOMO (E_{0-0}(S*) + E_{red} (S/S$^-$)) levels from 1.36 V for zzx-op1 and 1.22 V for zzx-op2 to 1.15 V for zzx-op3.[40] In p-type DSCs, the reduced sensitizers were oxidized by the electrolyte. The redox potential of E(I_3^-/ $I_2^{\bullet-}$) ≈ −0.19 V vs NHE), which is more positive than the E_{red} (S/S$^-$) level of dyes zzx-op1-op3. This difference will afford thermodynamically favorable driving force for effective regeneration of dyes in p-type DSCs.[16] The dye regeneration driving forces can be determined according to the equation: ΔG_{reg}= e[E(M/M$^-$) − E_{red}(S/S$^-$)], E(I_3^-/$I_2^{\bullet-}$) = −0.19 V vs NHE. It was found the zzx-op1-op3 showed nearly identical dye regeneration driving force (−0.66, −0.63, −0.62 eV for zzx-op1, zzx-op2, and zzx-op3, respectively).[16] Hence, the higher J_{SC} and IPCE for zzx-op1 sensitized solar cells were attributed to the higher Φ_{inj}.[28]

Hole Injection Quantum Yield. The energy conversion efficiency can be best described by IPCE. In eq 1, the LHE can be calculated using following equation:[52] LHE = 1−10^{-A}, in which A is the absorbance of the photoelectrode and can be estimated from the absorption spectra of dye-sensitized NiO film (2.3 μm thickness) as shown in Figure S1 in the Supporting Information. The maximal LHE of the devices are 73.8% at 525 nm (zzx-op1), 75.1% at 535 nm (zzx-op2), and 76.2% at 545 nm (zzx-op3), respectively. The charge collection efficiency η_{coll} obtained from transient photovoltage decay measurements also increased slightly from 62.1 (zzx-op1), 67.7 (zzx-op2), to 69.6% (zzx-op3) at 1 Sun illumination. It was found the calculated Φ_{inj} values were very different for three zzx-op dyes. The Φ_{inj} decreased in the order of zzx-op1 (90.3%) > zzx-op2 (53.9%) > zzx-op3 (39.0%). This is in consistent with the energy conversion efficiency of three dyes. Considering that three dyes exhibited identical dye-regeneration driving force and the same interfacial charge recombination process at the NiO/dye/electrolyte interface of the devices based on these dyes, the different energy conversion efficiency of three dyes originated from their different charge injection efficiency. In our case, it is likely that ∼0.80 ev of hole injection driving force is needed to achieve relatively high hole injection quantum yield.

3. CONCLUSIONS

p-Type DSCs have potentials to form tandem structures with n-type DSCs to capture and convert photons in different energy to electricity. However, the further development is limited by their poor photovoltaic performance. In this study, we synthesized a series of diphenylamine-fluorene based organic dyes and studied the how the linkers affect the photophysical and electrochemical properties in the devices. We found when the linker changed from a single fluorene to the combination with 3,4-ethylenedioxythiophene and thiophene units, the absorption maximum gradually shifted to the longer wavelengths, but the energy conversion efficiency decreased from 0.184, 0.160, to 0.153%. The dye loading study, transient photovoltage decay measurements and electrochemical impedance study indicated that this difference originated from different charge injection quantum yield, which was 90.3, 53.9, and 39.0% for zzx-op1, zzx-op2, and zzx-op3, respectively. We further found insertion of electron-rich heterocyclic aromatic groups 3,4-ethylenedioxythiophene and thiophene lifted the HOMO energy levels and decreased the driving forces for the hole injection. It is likely that ∼0.80 eV of hole injection driving force is needed to achieve relatively high hole injection quantum yield for NiO based p-type DSCs. Our investigation demonstrated that HOMO level of p-type dye plays a significant role on devices performance of p-type DSCs.

■ ASSOCIATED CONTENT

Supporting Information

Synthetic procedures and characterization data of all new compounds, emission spectra, absorption spectra on NiO nanoparticles, Cyclic voltammogram, and EIS data. This material is available free of charge via the Internet at http://pubs.acs.org.

■ AUTHOR INFORMATION

Corresponding Authors

*E-mail: zhixin-zhao@hust.edu.cn.
*E-mail: wnlochenwei@hust.edu.cn.
*E-mail: hhe@eiu.edu.

Author Contributions

The manuscript was written through contributions of all authors. All authors have given approval to the final version of the manuscript.

Notes

The authors declare no competing financial interest.

■ ACKNOWLEDGMENTS

This work was partially supported by the National Basic Research Program of China (973 program), Grant 2011CBA00703, the Fundamental Research Funds for the Central Universities, Grant HUST: 2012QN108 (Z.Z.), and Eastern Illinois University The Council on Faculty Research Grant (H.H.). Q.A. acknowledges a Swinburne University Postgraduate Research Award (SUPRA) and F.W. thanks the National Computational Infrastructure (NCI) at the Australian National University under the Merit Allocation Scheme (MAS)

and Swinburne University Supercomputing Facilities (Green/gSTAR) for computer resources.

REFERENCES

(1) O'Regan, B.; Grätzel, M. *Nature* **1991**, 737−740.
(2) Hagfeldt, A.; Boschloo, G.; Sun, L.; Kloo, L.; Pettersson, H. *Chem. Rev.* **2010**, *110*, 6595−6663.
(3) Grätzel, M. *Acc. Chem. Res.* **2009**, *42*, 1788−1798.
(4) Li, L.; Diau, E. W. *Chem. Soc. Rev.* **2013**, *42*, 291−304.
(5) O'Regan, B. C.; Durrant, J. R. *Acc. Chem. Res.* **2009**, *42*, 1799−1808.
(6) Yella, A.; Lee, H.; Hoi Nok Tsao, C. Y.; Chandiran, A. K.; Nazeeruddin, M. K.; Diau, E. W.; Yeh, C.; Zakeeruddin, S. M.; Grätzel, M. *Science* **2011**, *334*, 629−634.
(7) Odobel, F.; Le Pleux, L.; Pellegrin, Y.; Blart, E. *Acc. Chem. Res.* **2010**, *43*, 1063−1071.
(8) Nattestad, A.; Mozer, A. J.; Fischer, M. K. R.; Cheng, Y. B.; Mishra, A.; Bäuerle, P.; Bach, U. *Nat. Mater.* **2010**, *9*, 31−35.
(9) Odobel, F.; Pellegrin, Y.; Gibson, E. A.; Hagfeldt, A.; Smeigh, A. L.; Hammarström, L. *Coord. Chem. Rev.* **2012**, *256*, 2414−2423.
(10) He, J.; Lindström, H.; Hagfeldt, A.; Lindquist, S. *Sol. Energy Mater. Sol.* **2000**, *62*, 265−273.
(11) Yamada, K.; Fukuda, R.; Yamamoto, K.; Sonoda, T.; Nakamura, H.; Yamane, H. *Mol. Cryst. Liq. Cryst.* **2012**, *566*, 193−201.
(12) He, J.; Lindström, H.; Hagfeldt, A.; Lindquist, S. *J. Phys. Chem. B* **1999**, *103*, 8940−8943.
(13) Morandeira, A.; Fortage, J.; Edvinsson, T.; Le Pleux, L.; Blart, E.; Boschloo, G.; Hagfeldt, A.; Hammarström, L.; Odobel, F. *J. Phys. Chem. C* **2008**, *112*, 1721−1728.
(14) Le Pleux, L.; Smeigh, A. L.; Gibson, E.; Pellegrin, Y.; Blart, E.; Boschloo, G.; Hagfeldt, A.; Hammarström, L.; Odobel, F. *Energy Environ. Sci.* **2011**, *4*, 2075−2084.
(15) Favereau, L.; Warnan, J.; Pellegrin, Y.; Blart, E.; Boujtita, M.; Jacquemin, D.; Odobel, F. *Chem. Commun.* **2013**, *49*, 8018−8020.
(16) Gibson, E. A.; Le Pleux, L.; Fortage, J.; Pellegrin, Y.; Blart, E.; Odobel, F.; Hagfeldt, A.; Boschloo, G. *Langmuir* **2012**, *28*, 6485−6493.
(17) Gibson, E. A.; Smeigh, A. L.; Le Pleux, L.; Fortage, J.; Boschloo, G.; Blart, E.; Pellegrin, Y.; Odobel, F.; Hagfeldt, A.; Hammarström, L. *Angew. Chem., Int. Ed.* **2009**, *48*, 4402−4405.
(18) Gibson, E. A.; Smeigh, A. L.; Le Pleux, L.; Hammarström, L.; Odobel, F.; Boschloo, G.; Hagfeldt, A. *J. Phys. Chem. C* **2011**, *115*, 9772−9779.
(19) Qin, P.; Zhu, H.; Edvinsson, T.; Boschloo, G.; Hagfeldt, A.; Sun, L. *J. Am. Chem. Soc.* **2008**, *130*, 8570−8571.
(20) Li, L.; Gibson, E. A.; Qin, P.; Boschloo, G.; Gorlov, M.; Hagfeldt, A.; Sun, L. *Adv. Mater.* **2010**, *22*, 1759−1762.
(21) Qin, P.; Linder, M.; Brinck, T.; Boschloo, G.; Hagfeldt, A.; Sun, L. *Adv. Mater.* **2009**, *21*, 2993−2996.
(22) Yen, Y.; Chen, W.; Hsu, C.; Chou, H.; Lin, J. T.; Yeh, M. P. *Org. Lett.* **2011**, *13*, 4930−4933.
(23) Chang, C.; Chen, Y.; Hsu, C.; Chou, H.; Lin, J. T. *Org. Lett.* **2012**, *14*, 4726−4729.
(24) Ji, Z.; Natu, G.; Huanga, Z.; Wu, Y. *Energy Environ. Sci.* **2011**, *4*, 2818−2821.
(25) Powar, S.; Wu, Q.; Weidelener, M.; Nattestad, A.; Hu, Z.; Mishra, A.; Bäuerle, P.; Spiccia, L.; Cheng, Y.; Bach, U. *Energy Environ. Sci.* **2012**, *5*, 8896−8900.
(26) Zhang, X. L.; Zhang, Z.; Chen, D.; Bäuerle, P.; Bach, U.; Cheng, Y. *Chem. Commun.* **2012**, *48*, 9885−9887.
(27) Powar, S.; Daeneke, T.; Ma, M. T.; Dongchuan, F.; Duffy, N. W.; Götz, G.; Weidelener, M.; Mishra, A.; Bäuerle, P.; Spiccia, L.; Bach, U. *Angew. Chem., Int. Ed.* **2013**, *52*, 602−605.
(28) Borgström, M.; Blart, E.; Boschloo, G.; Mukhtar, E.; Hagfeldt, A.; Hammarström, L.; Odobel, F. *J. Phys. Chem. B* **2005**, *109*, 22928−22934.
(29) Morandeira, A.; Boschloo, G.; Hagfeldt, A.; Hammarström, L. *J. Phys. Chem. B* **2005**, *109*, 19403−19410.
(30) Mori, S.; Fukuda, S.; Sumikura, S.; Takeda, Y.; Tamaki, Y.; Suzuki, E.; Abe, T. *J. Phys. Chem. C* **2008**, *112*, 16134−16139.
(31) Sara, E.; Koops; Brian, C. O; Regan; Piers, R. F.; Barnes; James, R.; Durrant. *J. Am. Chem. Soc.* **2009**, *131*, 4808−4818.
(32) Nguyen, W. H.; Bailie, C. D.; Burschka, J.; Moehl, T.; Grätzel, M.; McGehee, M. D.; Alan, S. *Chem. Mater.* **2013**, *25*, 1519−1525.
(33) Li, C.; Liu, M.; Pschirer, N. G.; Baumgarten, M.; Müllen, K. *Chem. Rev.* **2010**, *110*, 6817−6855.
(34) Zeng, W.; Cao, Y.; Bai, Y.; Wang, Y.; Shi, Y.; Zhang, M.; Wang, F.; Pan, C.; Wang, P. *Chem. Mater.* **2010**, *22*, 1915−1925.
(35) Xu, M.; Wenger, S.; Bala, H.; Shi, D.; Li, R.; Zhou, Y.; Zakeeruddin, S. M.; Grätzel, M.; Wang, P. *J. Phys. Chem. C* **2009**, *113*, 2966−2973.
(36) Abbotto, A.; Calderon, E. H.; Dangate, M. S.; De Angelis, F.; Manfredi, N.; Mari, C. M.; Marinzi, C.; Mosconi, E.; Muccini, M.; Ruffo, R.; Seri, M. *Macromolecules* **2010**, *43*, 9698−9713.
(37) Bai, Y.; Zhang, J.; Zhou, D.; Wang, Y.; Zhang, M.; Wang, P. *J. Am. Chem. Soc.* **2011**, *133*, 11442−11445.
(38) Moon, S.; Yum, J.; Humphry-Baker, R.; Karlsson, K. M.; Hagberg, D. P.; Marinado, T.; Hagfeldt, A.; Sun, L.; Grätzel, M.; Nazeeruddin, M. K. *J. Phys. Chem. C* **2009**, *113*, 16816−16820.
(39) Meager, I.; Ashraf, R. S.; Mollinger, S.; Schroeder, B. C.; Bronstein, H.; Beatrup, D.; Vezie, M. S.; Kirchartz, T.; Salleo, A.; Nelson, J.; McCulloch, I. *J. Am. Chem. Soc.* **2013**, *135*, 11537−11540.
(40) Preat, J.; Hagfeldt, A.; Perpète, E. A. *Energy Environ. Sci.* **2011**, *4*, 4537−4549.
(41) Weidelener, M.; Mishra, A.; Nattestad, A.; Powar, S.; Mozer, A. J.; Mena-Osteritz, E.; Cheng, Y.; Bach, U.; Bäuerle, P. *J. Mater. Chem.* **2012**, *22*, 7366−7379.
(42) Paek, S.; Choi, H.; Choi, H.; Lee, C.; Kang, M.; Song, K.; Nazeeruddin, M. K.; Ko, J. *J. Phys. Chem. C* **2010**, *114*, 14646−14653.
(43) Zhao, Y.; Jiang, K.; Xu, W.; Zhu, D. *Tetrahedron* **2012**, *68*, 9113−9118.
(44) Cai, N.; Li, R.; Wang, Y.; Zhang, M.; Wang, P. *Energy Environ. Sci.* **2012**, *6*, 139−147.
(45) Huang, Z.; Natu, G.; Ji, Z.; Hasin, P.; Wu, Y. *J. Phys. Chem. C* **2011**, *115*, 25109−25114.
(46) Wang, Q.; Moser, J.; Grätzel, M. *J. Phys. Chem. B* **2005**, *109*, 14945−14953.
(47) O'Regan, B. C.; Bakker, K.; Kroeze, J.; Smit, H.; Sommeling, P.; Durrant, J. R. *J. Phys. Chem. B* **2006**, *110*, 17155−17160.
(48) Bai, J.; Xu, X.; Xu, L.; Cui, J.; Huang, D.; Chen, W.; Cheng, Y.; Shen, Y.; Wang, M. *ChemSusChem* **2013**, *6*, 622−629.
(49) Bisquert, J.; Zaban, A.; Greenshtein, M.; Mora-Seró, I. *J. Am. Chem. Soc.* **2004**, *126*, 13550−13559.
(50) Barone, V.; Cossi, M. *J. Phys. Chem. A* **1998**, *102*, 1995−2001.
(51) Selvam, L.; Vasilyev, V.; Wang, F. *J. Phys. Chem. B* **2009**, *113*, 11496−11504.
(52) Nazeeruddin, M. K.; A. Kay, I. R.; Humphry-Baker, R.; E. Mueller, P. L.; Vlachopoulos, N.; M., G. *J. Am. Chem. Soc.* **1993**, *115*, 6382−6390.